Appl. Phys. B 35, 237–241 (1984)

Applied Physics B Photophysics and Laser Chemistry

Phase Coherent Effects in a Collisional Turbulent Plasma

J. A. Johnson III

Department of Physics, The City College, CUNY, New York, NY 10031, USA

R. Ramaiah*

Department of Physics, Rutgers University, New Brunswick, NJ 08903, USA

Received 20 July 1983/Accepted 14 June 1984

Abstract. Stochastic fluctuations in a glow-discharge tube show typical turbulent spectra, mode-mode coupling, and evidence of pronounced three-dimensionality.

PACS: 52.35 Ra, 52.25 Gj, 51.50 +v

Several investigators have discussed the general importance of phase-coherent fluctuations in turbulent non-collisionless plasmas [1–8]. Some measurements have been made on ionization waves; however, little attention has been given to the unique role which nonlinear interactions might play in completely unstable environments. We have begun to address this issue [9, 10]. Here, we report on the presence of mode-mode coupling in turbulent fluctuations in the positive colum of a glow discharge in argon.

1. Experimental Procedures and Analytical Techniques

Our measurements were performed in a Pyrex glass tube of 80 cm length and 2.5 cm inner diameter. Thermally emitted electrons assisted the discharge process and we were able to obtain the positive column at 15 cm from the cathode. The general layout is given in Figs. 1 and 2.

The array of Langmuir probes was situated 40 cm from the cathode. Two of the three probes, biased into the ion saturation regime, monitor overall average values of plasma temperature and density. The probe bias system is shown in Fig. 3. The bias voltage is provided by a Gencom-Emitronics double polarity power supply. No ripple could be detected in the output of this supply. The circuits are shoelded in grounded aluminum boxes. The probes are mounted in vacuum quick-coupler housings and are constructed with a 0.75 mm diameter stainless steel wire, encased in a sheath of 1.5 mm o.d. Al_2O_3 ceramic insulator. One end of the probe is ground to a plane flush with the

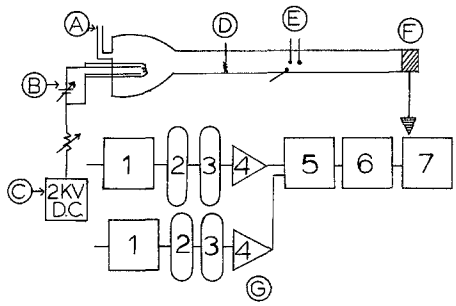

Fig. 1. Experimental setup. Shown are the vacuum port (A), thermionic cathode (B), power supply (C), grid exciter (D), probe array (E) and water cooled anode (F). A schematic of the data acquisition system is shown at (G): Probe biasing circuit (1); low-pass and high-pass filters (2, 3); amplifier HP-465A; A/D converter, biomation 8100 (5); data storage, Techran 951, (6); PDP-10 (7)

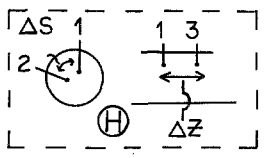

Fig. 2. Shown at (H) are the details of the probe array, azimuthal and axial arrangements: $\Delta\phi$ equals 0.6 rad and Δz equals 0.5 cm

* Present address: North American Philips Lighting Corp., Bath, NY

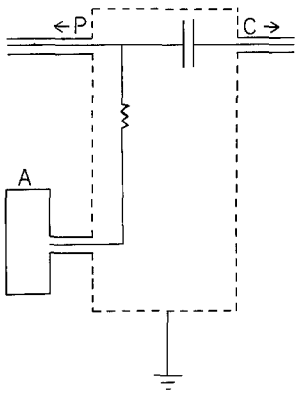

Fig. 3. Probe circuit. The probe bias at (A) is a double polarity GENCOM power supply. The resistance and capacitance are 50 kΩ and 0.25 μF, respectively. At (P) is the BNC connector to the probe; at (C) is the BNC connector to the data acquisition system

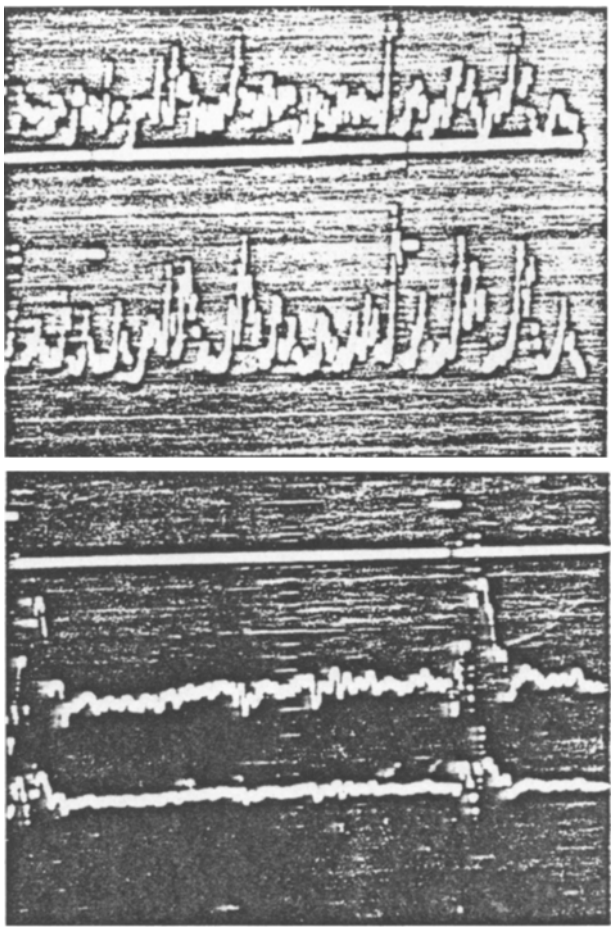

Fig. 4. Grid exciter effect. *Upper photograph:* Probe outputs are in the axial configuration with a pulse width (pw) of 0.1 ms, a repetition rate of 0.2 kHz, tube pressure of 100 mTorr in argon. *Lower photograph:* The conditions are the same as above with the exception that the tube pressure is 500 mTorr. Notice the absence of a noticeable grid effect at the lower pressure. At the higher pressure, the grid signal is clear and the plasma is also stable

sheath, the other end being soldered to BNC. The assembly is then inserted into a 1/4″ o.d. teflon rod, which allows positioning of the probe tip in the discharge. This configuration has the advantage of small local disturbance, high frequency response, good spatial resolution, and high insulator work function.

A grid, 2 cm in diameter and made of fine mesh steel wire, was inserted into the positive column 12 cm from the probe array. Pulses (80 V, 0.1 ms width) were applied to the grid at repetition rates of 0.2 and 7 kHz. Figure 4 shows the effect of the pulsed grid in Ar discharges at pressures of 100 and 500 mTorr. At 100 mTorr, the plasma exhibits the multimode structure that characterizes a turbulent state and the gird effects are not discernable; i.e., the probe outputs with and without grid excitation are the same in this case. At 500 mTorr, the plasma is quiescent (nonturbulent) and the plasma response to grid excitation is evident. Therefore, the range of pressures chosen for study here does exceed 100 mTorr, where there is no significant response to the grid excitations, and the grid served primarily to insure that an instability source existed in the positive column.

The probe outputs were passed through a series of filters in order to eliminate fluctuations above the Nyquist frequency of the analog to digital converter and those arising from 60 cycle noise. The resulting signals were digitized and stored at a rate such that several runs could be obtained during which the plasma parameters were essentially constant.

Familiar techniques [11–13] were used to determine the parameters of interest: 5he auto-power spectra P_{11}, P_{22}, and P_{33}; the cross power spectra P_{12} and P_{13}; phase spectra θ_{12} and θ_{13}; cross correlation functions C_{12} and C_{13}; and the bispectrum $b(k, l)$. The K behavior is obtained from the relation

$$K_{ij} = \theta_{ij} / \Delta r_{ij} .$$

Thus K_{12} would be the azimuthal wavenumber and K_{13} would be the axial wavenumber. The correlation time is defined as that time interval for which the time correlation coefficient C_{ij} decays by a factor e^{-1}. The bispectrum was computed by dividing the input (2048 points, sampling rate of 1 μs/sample) into 16 data sets of 128 points each. After subtracting the mean from each of these sets, a Hanning window was applied to each set and the bispectrum computed

$$b(k,l) = \frac{\left| \frac{1}{M} \sum_{i=1}^{M} X_k^{(i)} \cdot X_l^{(i)} \cdot X_{k+l}^{*(i)} \right|}{\left(\left| \frac{1}{M} \sum_{i=1}^{M} X_k^{(i)} \cdot X_l^{(i)} \right|^2 \right)^{1/2} \left(\frac{1}{M} \sum_{i=1}^{M} \left| X_{k=l} \right|^2 \right)^{1/2}}, \quad (1)$$

where $1 < k < N/4$; $k < l < [(N/2) - k]$; $N = 128$ and X_k are the Fourier amplitudes at frequency ω_k and

wavenumber K_k computed by our Fast Fourier Transform algorithm [14]. In this, $b(k, l)$ measures the phase coherence between modes of the system and takes on values close to one if the 3-wave resonance condition for non-linear wave-wave interaction is satisfied, i.e.,

$$\omega_k \pm \omega_1 = \omega_{k+1},$$
$$\mathbf{k}_k \pm \mathbf{k}_1 = k_{k+1}. \quad (2)$$

2. The Evidence of Coherence

These procedures were applied in detail to our set-up for a variety of discharge tube pressures. Typical power spectra are shown in Fig. 5. A dominant mode at $f = 125$ kHz can be seen in the outo-spectra of the two probes in the azimuthal plane. The corresponding cross spectrum shows dominant modes at $f = 31.5$, 62.5 and 125 kHz thereby indicating that a certain degree of rotational symmetry exits for these conditions. Turbulent plasma theories predict [15] that the power spectra should show a frequency dependency of the form $P \propto \omega^{-n}$. Figure 6 shows typical results qualitatively confirming the prediction for two runs which are representative of the range available to us. When auto-spectra at two locations separated axially are compared, we find that the high-frequency components tend to disappear which indicates longitudinal damping. Examination of the dispersion plots shows (Fig. 7) $K\alpha\omega$ up to roughly 375 kHz. For these cases where $K\alpha\omega$, the group velocities are 0.8×10^5 and 2×10^5 cm/s, a result which is in accord with the differeence in the spectral indices n.

In Figs. 8 and 9 are typical individual bispectrum plots. The procedure used is to fix a value of k and let l vary according to the restrictions in (2); thus we are in effect inspecting slices of the three-dimensional plot of $b(k, l)$.

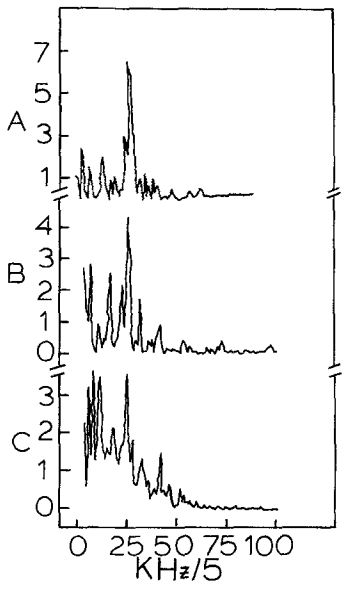

Fig. 5. The first trace (A) is a plot of the auto-power spectrum (P_{11}) vs. frequency (f), the second trace (B) is the plot of P_{22} vs. f for the probes in the azimuthal plane for the following operating conditions: $p = 50$ mTorr, discharge current $I_d = 100$ mA, discharge voltage $V_d = 0.3$ kV, $T_e = 1.8$ eV and $n_e \simeq 10^9$ cm^{-3}, grid pulse height (h) = 80 V, pulse width (pw) = 0.1 ms, repetition rate $r = 7$ kHz. The third trace (C) is the corresponding cross-power spectra (P_{12}) vs. f

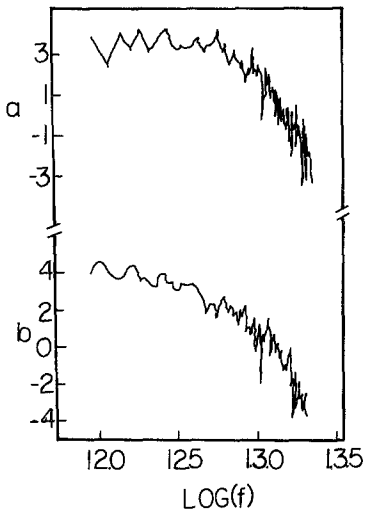

Fig. 6. The first trace is the plot of $\log(P_{12})$ vs. $\log(f)$ for the conditions of Fig. 5. The spectral index (see text) for this case is 5.08. The second trace is a plot of $\log(P_{13})$ vs.$\log(f)$ when the probes are in the axial arrangement. The operating conditions for this case are $p = 90$ mTorr, $I_d = 100$ mA, $V_d = 0.4$ kV, $T_e \simeq 1$ eV, $n_e \simeq 10^{10}$ cm^{-3}, $h = 80$ V, $pw = 0.1$ ms, $r = 0.2$ kHz. The spectral index foe this case is 4.71

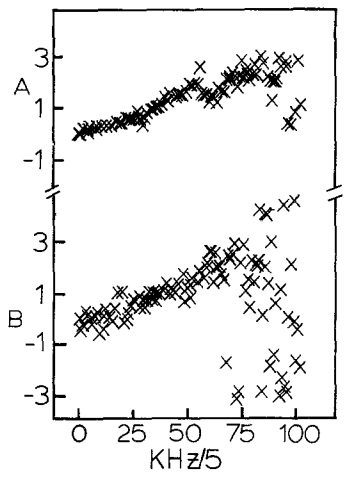

Fig. 7. Shown are the K plots for the axial (A) and azimuthal (B) probe arrangements. Trace A corresponds to the discharge conditions stated for the second trace in Fig. 6. Trace B corresponds to the discharge conditions discussed in Fig. 5. The group velocities computed from the traces are 0.8×10^5 and 2×10^5 cm/s, respectively

The corresponding power spectrum is shown in Fig. 10 and the identification of mode-mode coupling in the components is easily made. These data show that the three wave conditions are borne out well.

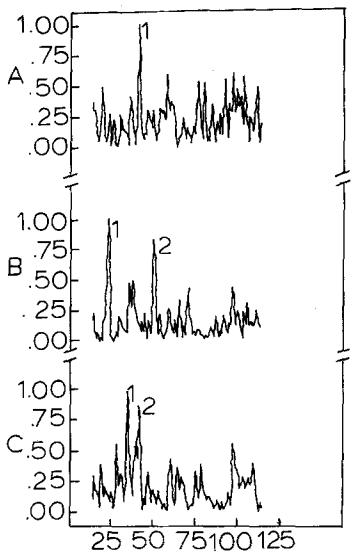

Fig. 8. Shown are three plots of $b^2(k, l)$ vs. f, obtained in the azimuthal probe arrangement, for three constant values of f_k as indicated, see text and (1). All peaks that had a value close to one were labelled $l(i)$ and their frequencies $f_{l(i)}$ determined. Then a check was made with Fig. 9 to determined if there were peaks at f_k, $f_{l(i)}$ and $f_{k+l(i)}$. Further the wave numbers corresponding to these peaks, k_k, $k_{l(i)}$, $k_{k+l(i)}$ were determined from Fig. 7. If these frequencies and wave numbers satisfied the three-wave resonance condition (see text), then a positive identification of a nonlinear interaction between mode at f_k and $f_{(i)}$ would be established. (i) *First trace:* $f_k = 36$ kHz; $f_{l(1)} = 184.3$ kHz; $f_{k+l(1)} = 220$ kHz, corresponds to f_A in trace *A* of Fig. 10. The wave numbers are $k_k = 0.14\,\mathrm{cm}^{-1}$, $k_{l(1)} = 0.66\,\mathrm{cm}^{-1}$ and $k_{k+l(1)} = 0.78\,\mathrm{cm}^{-1}$. As three-wave resonance conditions are satisfied, the mode at f_A is due to the nonlinear coupling of modes at f_k and $f_{l(1)}$. (ii) *Second trace:* $f_k = 58$ kHz, $f_{l(1)} = 80$ kHz, $f_{k+l(1)} = 138$ kHz, corresponds to f_B in trace A of Fig. 10. The wave numbers are $k_k = 0.21\,\mathrm{cm}^{-1}$, $k_{l(1)} = 0.29\,\mathrm{cm}^{-1}$, $k_{k+l(1)} = 0.52\,\mathrm{cm}^{-1}$. Three wave resonance conditions are satisfied and the mode at f_B is due to the nonlinear coupling of modes at f_k and $f_{l(1)}$. For the *second* peak, $f_k = 58$ kHz, $f_{l(2)} = 123.3$ kHz, $f_{k+l(2)} = 181.3$ kHz $= F_C$ in trace A of Fig. 10. The wave numbers are $k_k = 0.2\,\mathrm{cm}^{-1}$, $k_{l(2)} = 0.41\,\mathrm{cm}^{-1}$, $k_{k+l(2)} = 0.60\,\mathrm{cm}^{-1}$. Thus the mode at f_C is due to the coupling of modes at f_k and $f_{l(2)}$. For the *third* peak, $f_k = 58$ kHz, $f_{l(3)} = 256$ kHz, $f_{k+l(3)} = 314$ kHz $= fD$ in trace A of Fig. 10. The wave numbers are $k_k = 0.21\,\mathrm{cm}^{-1}$, $k_{l(3)} = 0.90\,\mathrm{cm}^{-1}$ and $k_{k+l(3)} = 1{,}22\,\mathrm{cm}^{-1}$. Hence the mode at f_D is due to the coupling of modes at fk and $f_{l(3)}$. (iii) *Third trace: First* peak, $f_k = 125$ kHz, $f_{l(1)} = 255$ kHz, $f_{k+l(1)} = 380$ kHz $= f_E$ in Fig. 5c. The wave number are $k_k = 0.45\,\mathrm{cm}^{-1}$, $k_{k(1)} = 0.94\,\mathrm{cm}^{-1}$, $k_{k+l(1)} = 1.4\,\mathrm{cm}^{-1}$. Thus the peak at f_E is due to the nonlinear coupling of peaks at f_k and $f_{l(1)}$. *Second* peak, $f_k = 125$ kHz, $f_{l(2)} = 307$ kHz, $f_{k+l(2)} = 432$ kHz $= f_F$ in Fig. 10. The wave numbers are $k_k = 0.45\,\mathrm{cm}^{-1}$, $k_{l(2)} = 1.1\,\mathrm{cm}^{-1}$ and $k_{k+l(2)} = 1.62\,\mathrm{cm}^{-1}$. The peak at f_F is due to the nonlinear coupling of f_k and $fl_{(2)}$. *Third* peak, $f_k = 125$ kHz, $f_{l(3)} = 320$ kHz, $f_{k+l(3)} = 445$ kHz $= fG$ in Fig. 5c. The wave numbers are $kk = 0.45\,\mathrm{cm}^{-1}$, $k_{l(3)} = 1.2\,\mathrm{cm}^{-1}$, $k_{k+l(3)} = 1.61\,\mathrm{cm}^{-1}$. The peak at f_G is due to nonlinear coupling of modes at f_k and $f_{l(3)}$

In Fig. 11, we show the overall variation of cross correlation times with pressure. At the lower pressure, azimuthal correlation times are less than one-half the corresponding axial values. However, above

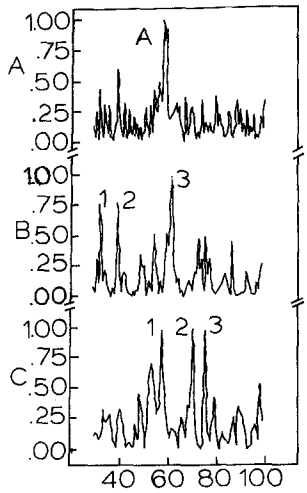

Fig. 9. Shown are three plots of $b^2(k, l)$ vs. f, in the axial probe arrangement, for three constant values of f_k. (i) *First trace:* $f_k = 36$ kHz, $f_{l(1)} = 143.3$ kHz, $f_{k+l(1)} = 179.3$ kHz $= f_A$ in trace B of Fig. 10. The wave numbers are $k_k = 0.38\,\mathrm{cm}^{-1}$, $k_{l(1)} = 1.5\,\mathrm{cm}^{-1}$, $k_{k+l(1)} = 2.0\,\mathrm{cm}^{-1}$. Thus the peak at f_A is due to nonlinear coupling of modes at f_k and $f_{l(1)}$. (ii) *Second trace: First* peak, $f_k = 41$ kHz, $f_{l(1)} = 80$ kHz, $f_{k+l(1)} = 121$ kHz $= f_B$ in trace B of Fig. 10. The wave numbers are $k_k = 0.42\,\mathrm{cm}^{-1}$, $k_{l(1)} = 0.84\,\mathrm{cm}^{-1}$, $k_{k+l(1)} = 1.28\,\mathrm{cm}^{-1}$. Thus the peak at f_B is due to the nonlinear coupling of modes at f_k and $f_{l(2)}$. *Second* peak, $f_k = 41$ kHz, $f_{l(2)} = 195$ kHz, $f_{k+l(2)} = 236$ kHz $= f_C$ in trace B of Fig. 10. The wave numbers are $k_k = 0.42\,\mathrm{cm}^{-1}$, $k_{l(2)} = 2.1\,\mathrm{cm}^{-1}$, $k_{k+l(2)} = 2.5\,\mathrm{cm}^{-1}$. The peak at f_C is due to nonlinear coupling of modes at f_k and $f_{l(2)}$. (iii) *Third trace: First* peak, $f_k = 56$ kHz, $f_{l(1)} = 143.3$ kHz, $f_{k+l(1)} = 199.3$ kHz $= f_D$ in trace B of Fig. 10. The wave numbers are $k_k = 0.6\,\mathrm{cm}^{-1}$. Thus the peak at f_D is due to nonlinear coupling of modes at f_k and $f_{l(1)}$. *Second* peak, $fk = 56$ kHz, $f_{l(2)} = 1.74\,\mathrm{cm}^{-1}$, $k_{k+l(2)} = 2.3\,\mathrm{cm}^{-1}$. Thus the mode at f_E is due to the nonlinear coupling of modes at f_k and $f_{l(2)}$

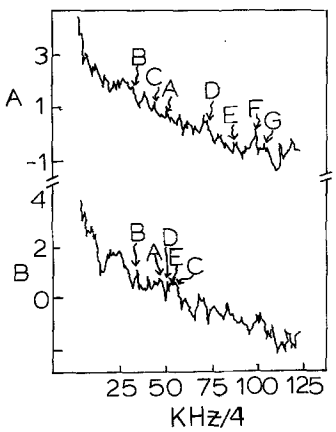

Fig. 10. Plots of the log of auto-power spectrum vs. frequency (f) for the azimuthal (trace A) and the axial (trace B) probe arrangements. The peaks indicated have been shown to be (partially) due to nonlinear wave-wave interactions

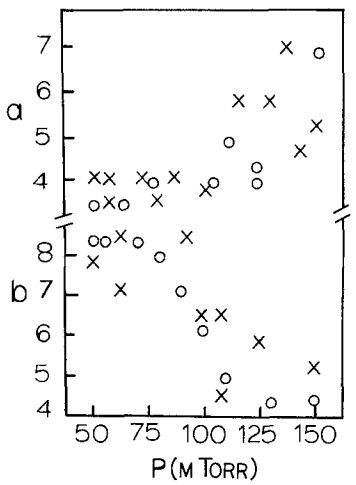

Fig. 11. The variation of cross-correlation time with gas pressure. The two grid excitation frequencis used are represented by $X=0.2$ kHz; $O=7$ kHz. Trace (a) is for the azimuthal probe arrangement and trace (b) is for the axial probe arrangement

100 mTorr there is a systematic increase in the former and decrease in the latter with increasing pressure. The turbulent system evolves into a set of axially localized structures; i.e., the characterizing wavelengths have become comparable to the probe spacing along the axis.

3. Conclusions

While plasma conditions in electric discharges are capable of sustaining several types of instabilities, the conditions required for the occurrence of ionization instability are often the most easily satisfied. Grabec and others [3, 16, 17] have associated these ionization instabilities with the appearance of ionization waves in the positive column of a glow discharge; specifically Grabec and Mikac [5] suggest that harmonic generation and mode-mode coupling play a significant role in the development of turbulence. Our results are directly relevant to these theoretical speculations. We have shown that mode coupling indeed occurs in our turbulent Ar discharge, in support of Grabec's treatment, and affirm that ionization instability appears to be the primary cause of this turbulence.

The spectral index measurements show that the fluctuations in a positive column are clearly turbulent-like. The phase spectra indicate that the system is nearly linear at low frequency. However, the bispectrum plots show that nonlinear wave-wave interactions play a major role in the development of the prominent fluctuation components in the turbulent spectrum. Furthermore, we are able tommake clear distinctions between the azimuthal and axial behaviors of the fluctuations. Our results imply a trend toward longer azimuthal scales and shorter axial scales for characterizing fluctuation wave-packets as the density of the turbulent environment increases. Therefore, we conclude that a realistic treatment of any comparable system must take into account the fact that the fluctuations are indeed turbulent but have inherently nonlinear phase coherent aspects. In addition, it is clear that the axial and azimuthal components are inter-related; a one-dimensional treatment is thus of little value.

Acknowledgements. This research was supported in part by grants SER-810430 from NSF and NAG-1-293 from NASA.

References

1. M. Porkalob, R.P.H. Chang: Rev. Mod. Phys. **50**, 745 (1978)
2. A.S. Monin: Sov. Phys. Usp. **21**, 429 (1978)
3. L. Pekarek: Sov. Phys. Usehki **11**, 188 (1968)
   L. Pekarek, Proc. 10th Intern. Conf. Ionization Phenomena in Gases (Springer, Berlin, Heidelberg, New York 1971) pp. 351–379
4. R. Haas: Phys. Rev. A**8**, 1017 (1973)
5. I. Grabec, S. Mikac: Plasma Phys. **16**, 1155 (1974)
6. A.B. Stewart: J. Appl. Phys. **27**, 911 (1956)
7. I. Grabec, S. Poberaj: Plasma Phys. **11**, 519 (1969)
8. K. Ohe, S. Takeda: Jpn. J. Appl. Phys. **11**, 1173 (1972) and **23**, 21 (1980)
9. J.A. Johnson III, J. Santiago, Lin I: Phys. Lett. **83**A, 443 (1981)
10. J.A. Johnson III, R. Ramaiah, J.P. Santiago: Rev. Sci. Inst. **52**, 936 (1981)
11. D.E. Smith, E.J. Powers, G.S. Caldwell: IEEE Trans. PS-**2**, 261 (1974)
12. K.F. Shoenberg: Rev. Sci. Instrum. **51**, 1151 (1980)
13. Y.C. Kim, J.M. Beall, E.J. Powers, R.W. Miksa: Phys. Fluids **23**, 258 (1980)
14. H.J. Nussbaumer: Fast Fourier Transform and Convolution Algorithm, 2nd ed., Springer Ser. Inf. Sci. **2** (Springer, Berlin, Heidelberg, New York 1982)
15. J.R. Roth: Phys. Fluids **14**, 2193 (1971)
16. I. Grabec: Phys. Fluids **17**, 10 (1974)
17. W.L. Nighan, W.J. Weigand, R.A. Hass: Appl. Phys. Lett. **22**, 579 (1973)